SANTA CRUZ BIOTECHNOLOGY, INC.

ACSL4 (F-4): sc-365230

SANTA CRUZ BIOTECHNOLOGY

The Power to Question

BACKGROUND

Acyl-CoA synthetases, also known as long-chain fatty-acid CoA synthases (FACL) or palmitoyl-CoA ligases, include ACSL1-6, which are all single-pass membrane proteins localizing to the mitochondrion, microsome or peroxisome. ACSL proteins are important for synthesis of cellular lipids and for β-oxidation degradation. Specifically, ACSL proteins catalyze the activation of long-chain fatty acids to acyl-CoAs, which can be metabolized to form CO_2, triacylglycerol (TAG), phospholipids (PL) and cholesteryl esters (CE). ACSL3 preferentially utilizes laurate, myristate, arachidonate and eicosapentaenoate among saturated and unsaturated long chain fatty acids. FACL3 is expressed as two isoforms in various tissues, including brain, heart, placenta, prostate, skeletal muscle, testis and thymus. FACL4 preferentially utilizes arachidonate and is abundant in steroidogenic tissues. FACL4 may modulate female fertility and uterine prostaglandin production.

CHROMOSOMAL LOCATION

Genetic locus: ACSL4 (human) mapping to Xq23; Acsl4 (mouse) mapping to X F2.

SOURCE

ACSL4 (F-4) is a mouse monoclonal antibody raised against amino acids 623-675 mapping near the C-terminus of ACSL4 of human origin.

PRODUCT

Each vial contains 200 µg IgG_1 kappa light chain in 1.0 ml of PBS with < 0.1% sodium azide and 0.1% gelatin.

ACSL4 (F-4) is available conjugated to agarose (sc-365230 AC), 500 µg/0.25 ml agarose in 1 ml, for IP; to HRP (sc-365230 HRP), 200 µg/ml, for WB, IHC(P) and ELISA; to either phycoerythrin (sc-365230 PE), fluorescein (sc-365230 FITC), Alexa Fluor® 488 (sc-365230 AF488), Alexa Fluor® 546 (sc-365230 AF546), Alexa Fluor® 594 (sc-365230 AF594) or Alexa Fluor® 647 (sc-365230 AF647), 200 µg/ml, for WB (RGB), IF, IHC(P) and FCM; and to either Alexa Fluor® 680 (sc-365230 AF680) or Alexa Fluor® 790 (sc-365230 AF790), 200 µg/ml, for Near-Infrared (NIR) WB, IF and FCM.

APPLICATIONS

ACSL4 (F-4) is recommended for detection of short isoform and long isoform of ACSL4 of mouse, rat and human origin by Western Blotting (starting dilution 1:100, dilution range 1:100-1:1000), immunoprecipitation [1-2 µg per 100-500 µg of total protein (1 ml of cell lysate)], immunofluorescence (starting dilution 1:50, dilution range 1:50-1:500), immunohistochemistry (including paraffin-embedded sections) (starting dilution 1:50, dilution range 1:50-1:500) and solid phase ELISA (starting dilution 1:30, dilution range 1:30-1:3000).

Suitable for use as control antibody for ACSL4 siRNA (h): sc-60619, ACSL4 siRNA (m): sc-60620, ACSL4 shRNA Plasmid (h): sc-60619-SH, ACSL4 shRNA Plasmid (m): sc-60620-SH, ACSL4 shRNA (h) Lentiviral Particles: sc-60619-V and ACSL4 shRNA (m) Lentiviral Particles: sc-60620-V.

Molecular Weight of ACSL4: 75 kDa.

Positive Controls: Caco-2 cell lysate: sc-2262, HEK293T whole cell lysate: sc-45137 or HeLa whole cell lysate: sc-2200.

STORAGE

Store at 4° C, **DO NOT FREEZE**. Stable for one year from the date of shipment. Non-hazardous. No MSDS required.

DATA

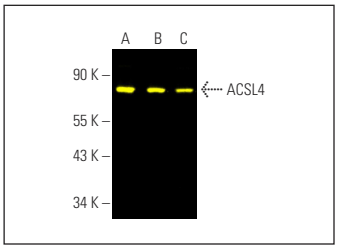

ACSL4 (F-4) Alexa Fluor® 488: sc-365230 AF488. Direct fluorescent western blot analysis of ACSL4 expression in HeLa (**A**), Caco-2 (**B**) and HEK293T (**C**) whole cell lysates. Blocked with UltraCruz® Blocking Reagent: sc-516214.

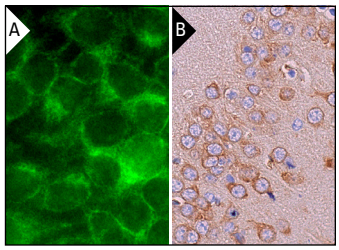

ACSL4 (F-4): sc-365230. Immunofluorescence staining of formalin-fixed HeLa cells showing mitochondrial localization (**A**). Immunoperoxidase staining of formalin fixed, paraffin-embedded mouse brain tissue showing cytoplasmic staining of neuronal cells (**B**).

SELECT PRODUCT CITATIONS

1. Herrera-Martínez, M., et al. 2013. Actin, RhoA, and Rab11 participation during encystment in *Entamoeba invadens*. Biomed Res. Int. 2013: 919345.
2. Xu, W.D., et al. 2015. Up-regulation of fatty acid oxidation in the ligament as a contributing factor of ankylosing spondylitis: a comparative proteomic study. J. Proteomics 113: 57-72.
3. Radif, Y., et al. 2018. The endogenous subcellular localisations of the long chain fatty acid-activating enzymes ACSL3 and ACSL4 in sarcoma and breast cancer cells. Mol. Cell. Biochem. 448: 275-286.
4. Wen, Q., et al. 2019. The release and activity of HMGB1 in ferroptosis. Biochem. Biophys. Res. Commun. 510: 278-283.
5. Shah, S.S., et al. 2019. APOL1 kidney risk variants induce cell death via mitochondrial translocation and opening of the mitochondrial permeability transition pore. J. Am. Soc. Nephrol. 30: 2355-2368.
6. Tao, P., et al. 2020. A dominant autoinflammatory disease caused by non-cleavable variants of RIPK1. Nature 577: 109-114.
7. Kapralov, A.A., et al. 2020. Redox lipid reprogramming commands susceptibility of macrophages and microglia to ferroptotic death. Nat. Chem. Biol. 16: 278-290.
8. Feng, H., et al. 2020. Transferrin receptor is a specific ferroptosis marker. Cell Rep. 30: 3411-3423.e7.
9. NavaneethaKrishnan, S., et al. 2020. mPTP opening caused by Cdk5 loss is due to increased mitochondrial Ca^{2+} uptake. Oncogene 39: 2797-2806.
10. Wang, C., et al. 2020. Different regions of synaptic vesicle membrane regulate VAMP2 conformation for the SNARE assembly. Nat. Commun. 11: 1531.

RESEARCH USE

For research use only, not for use in diagnostic procedures.